energies

MDPI

Article

A Glowworm Swarm Optimization-Based Maximum Power Point Tracking for Photovoltaic/Thermal Systems under Non-Uniform Solar Irradiation and Temperature Distribution

Yi Jin [1], Wenhui Hou [1], Guiqiang Li [2,*] and Xiao Chen [3]

[1] Department of Precision Machinery and Precision Instrumentation, University of Science and Technology of China, 96 Jinzhai Road, Hefei 230036, China; jinyi08@ustc.edu.cn (Y.J.); houwh009@gmail.com (W.H.)
[2] Department of Thermal Science and Energy Engineering, University of Science and Technology of China, 96 Jinzhai Road, Hefei 230026, China
[3] State Key Laboratory of Fire Science, University of Science and Technology of China, 96 Jinzhai Road, Hefei 230026, China; summercx@mail.ustc.edu.cn
* Correspondence: ligq@mail.ustc.edu.cn; Tel./Fax: +86-551-6360-3512

Academic Editor: Tapas Mallick
Received: 19 January 2017; Accepted: 11 April 2017; Published: 15 April 2017

Abstract: The output power of a photovoltaic (PV) system depends on the external solar irradiation and its own temperature. In order to obtain more power from the PV system, the maximum power point tracking (MPPT) is necessary. However, when the PV is partially shaded, there will be multiple peaks in the power-current (P-I) curve. The conventional MPPT methods may be invalid due to falling into the local peak. In addition, in a photovoltaic-thermal (PV/T) system, the non-uniform temperature distribution on PV will also occur, which complicates the situation. This paper presents a MPPT method with glowworm swarm optimization (GSO) for PV in a PV/T system under non-uniform solar irradiation and temperature distribution. In order to study the performance of the proposed method, the conventional methods including the perturbation and observe algorithm (P and O), and the fractional open-circuit voltage technique (FOCVT) are compared with it in this paper. Simulation results show that the proposed method can rapidly track the real maximum power point (MPP) under different conditions, such as the gradient temperature distribution, the fast variable solar irradiation and the variable partial shading. The outcome indicates the proposed method has obvious advantages, especially the performance being superior to the conventional methods under the partial shading condition.

Keywords: maximum power point tracking (MPPT); glowworm swarm optimization (GSO); photovoltaic-thermal (PV/T); non-uniform solar irradiation; temperature distribution

1. Introduction

With the sharp increasing global demand for energy, the shortage of the conventional fossil fuels and environmental pollution are becoming more and more serious. Thus, renewable energy resources are paid more and more attention from scholars due to their easy accessibility to humankind around the world. Renewable energy is meeting, at present, 13.5% of the global energy demand [1]. In recent years, there has been a rapid development in solar photovoltaic power generation systems due to various advantages of solar energy, including limitlessness, zero production of pollution, noiselessness, and good reliability. The output power of photovoltaic (PV) depends on the external environment and its own temperature. Thus, maximum power point tracking (MPPT) technology is necessary to control and keep the PV system working at the maximum power point (MPP) under any conditions.

Many MPPT techniques have been proposed. The most commonly used are the fractional open-circuit voltage technology (FOCVT) [2], perturbation and observation (P and O) [3–6], and incremental conductance (IncCond) [7–9]. The P and O method and IncCond method usually implement the perturbation on the control variable to search the MPP based on the feedback of the output power. The main advantages of these two methods are that they are compatible with any PV module, require no information about the PV module, and are easily implemented. However, the selection of the perturbation step size is difficult to meet the demand of efficiency and precision at the same time. Thus, the variable step-size P and O MPPT technique is proposed. The performance of different variable step-size P and O MPPT techniques is compared by Chen et al. [10]. In addition, there will be multiple peaks in the P-I characteristic curve under the partial shading condition in actual applications. These conventional methods reach the local MPP, but cannot analyze and compare all peaks to determine the true MPP [11]. Many advanced methods using artificial intelligence are presented, including artificial neural networks (ANN) [12,13] and fuzzy logic (FLC) [14–16]. Kofinas proposed an intelligent MPPT control scheme based on a direct neural control (DNC), which consists of a single adaptive neuron and a hybrid learning mechanism [17]. However, these methods usually need an enormous volume of data for training, professional experience, or a complex leaning process.

Recently, bio-inspired algorithms have drawn considerable attention due to their excellent characteristics in dealing with the non-linear and stochastic optimization problems. Many algorithms, like genetic algorithms (GA) [18], particle swarm optimization (PSO) [19], and artificial bee colony (ABC) [20], have been utilized for MPPT application. Larbes et al. improved the performance of the FLC controller by using genetic algorithms (GA) for optimization [21]. Sundareswaran combined the PSO algorithm and the P and O algorithm for MPPT application of PV under the partial shading condition [22].

Glowworm swarm optimization (GSO) is a novel bionic algorithm for the optimization of multimodal functions. It is firstly proposed by Krishnanand and Ghose, who were inspired from the natural phenomenon that glowworms exchange information of searching for food with their peers in 2005 [23]. The GSO algorithm shows outstanding performance in finding the optimal solution for the multimodal functions but, at present, it is still rarely used in MPPT for PV. Considering the characteristic of multiple peaks in a P-I curve caused by the non-uniform solar irradiation conditions, GSO may be very suitable for MPPT. In addition, the photovoltaic-thermal energy (PV/T) system has the common phenomenon of the non-uniform temperature distribution on PV. Thus, the conditions are complex for PV/T under the non-uniform solar irradiation and temperature distribution. Currently, there are much fewer studies using GSO under these conditions.

Therefore, in this paper, the novel GSO algorithm is presented to track the PV maximum power point for the PV/T application. In addition, in order to study the performance of the proposed method, the P and O method and FOCVT method are compared with it under four different complex conditions. The results indicate that the novel algorithm GSO is suitable for PV/T MPPT applications under non-uniform solar irradiation and temperature distribution.

2. Characteristics of Solar Modules

2.1. PV Cell

The characteristic curve (the voltage-current curve and the power-current curve) of the solar cell is nonlinear. From the equivalent circuit in Figure 1 [24], the output characteristic of the PV cell is given by Equations (1)–(9):

$$I_{ph} - I_d - I_{sh} - I = 0 \quad (1)$$

where I_{sh} is the current of the parallel resistance and I_{ph} is the light-generated current, which is proportional to the given solar irradiation. It can be calculated by:

$$I_{ph} = [I_{sc} + \alpha \cdot (T_c - T_r)] \cdot S/1000 \quad (2)$$

where I_{sc} is the short-circuit current at standard test condition (STC) ($T = 25\ ^{\circ}\mathrm{C}$, $S = 1000\,\mathrm{W/m^2}$) and α is the current temperature coefficient of the cell. T_c and T_r are the operating temperature and the reference temperature of the cell, respectively. I_d represents the diode current, which is given according to the Shockley equation:

$$I_d = I_O[\exp(qU_d/AkT_c) - 1] \quad (3)$$

where q is the electronic charge ($q = 1.6 \times 10^{-19}$), k is Boltzmann's constant ($k = 1.38 \times 10^{-23}$), A is the ideal factor of the diode, I_O is the reverse saturation current of the diode, where I_o varies with the change in temperature and is given by:

$$I_o = I_{ro}(T_c/T_r)^3 \exp[qE_g(1/T_c - 1/T_r)/Ak] \quad (4)$$

where E_g is the band gap energy of the semiconductor and I_{ro} is the saturation current of the diode at 25 °C, which is calculated by:

$$I_{ro} = I_{sc}/[\exp(qV_{oc}/AkT_r) - 1] \quad (5)$$

where V_{oc} is the open-circuit voltage of the PV module at STC ($T = 25^{\circ}\mathrm{C}$, $S = 1000\,\mathrm{W/m^2}$). U_d is the voltage of the equivalent diode which is given by:

$$U_d = U + IR_s \quad (6)$$

where R_s is the series resistance.

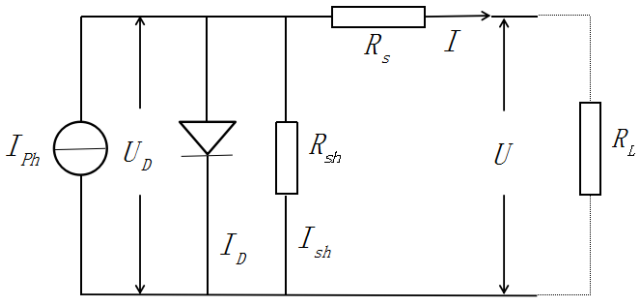

Figure 1. Equivalent circuit of the solar cell.

I_{sh} is the current of the parallel resistance, which is given by:

$$I_{sh} = (U + I \cdot R_s)/R_{sh} \quad (7)$$

where R_{sh} is the parallel resistance.

From the former analysis, the input-output characteristic of the PV cell is:

$$[I_{sc} + \alpha \cdot (T_c - T_r)] \cdot \frac{S}{1000} - I_o[\exp(\frac{q(U + I \cdot R_s)}{AkT_c}) - 1] - \frac{(U + I \cdot R_s)}{R_{sh}} - I = 0 \quad (8)$$

The output power of the PV cell is given by:

$$P = U \cdot I \quad (9)$$

The parameters values of the silicon solar cell used in simulation are illustrated in Table 1.

Table 1. Parameters of the silicon solar cell.

Parameters	Value	Unit
Current temp. coefficient	0.002086	A/°C
Open-circuit Voltage (V_{oc})	0.53	V
Short-circuit Current (I_{sc})	2.926	A
Ideal Factor (A)	1.3	-
Electrical resistance	0.0277	Ω

2.2. PV Module

The output power of one PV cell is limit, as shown in Figure 2. So in order to acquire the desired power, the PV cells are usually connected with each other in series and parallel. In this paper, the series mode is adopted. In PV/T application, there is the similar gradient temperature distribution on the PV module due to the heat exchange structure. The temperatures of the water inlet and the water outlet are different in photovoltaic-thermal (PV/T) systems. Thus, we assume that the temperature gradient scope is 0.2 °C. In the simulation, the temperature of the first cell is set to 20 °C, and the temperature gradient scope is 0.2 °C, as shown in Figure 3.

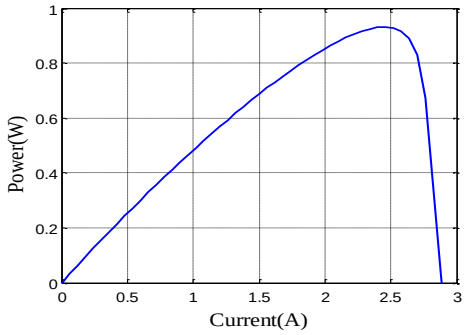

Figure 2. Output power of the photovoltaic (PV) cell.

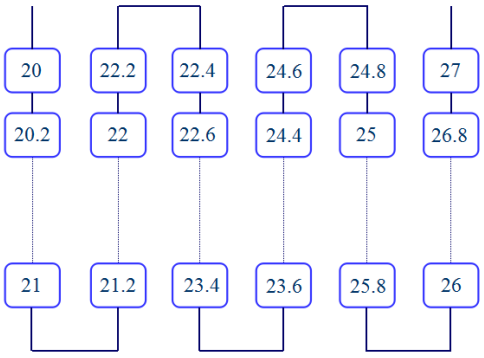

Figure 3. The ideal temperature distribution on PV for a photovoltaic-thermal (PV/T) system.

The P-I curves of the PV module under different solar irradiation is shown in Figure 4. This shows that the output power is a nonlinear function and is affected by the solar irradiation. Additionally, the electrical current corresponding to maximum power (I_{mp}) varies with the solar irradiation. Thus, in order to find the real I_{mp} as the reference operating point, the application of MPPT technology is necessary. The P-I curves of the PV module under different partial shading conditions is shown in Figure 5. The shading situation is shown in Figure 6. In this situation, the temperature distribution is assumed to be unaltered with Figure 3 since the shading area is small. The curves are characterized by multiple peaks in this condition. Most of the traditional MPPT methods usually may converge into

the LMPP (local maximum power point) instead of the global GMPP (global maximum power point). Thus, this paper applies the GSO algorithm to complete the MPPT.

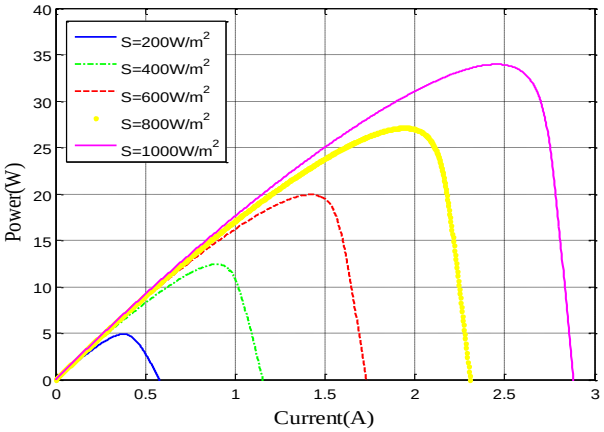

Figure 4. Output power of the PV module under different levels of solar irradiation.

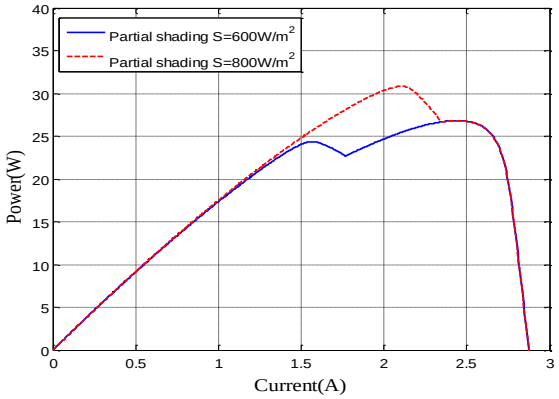

Figure 5. Output power of the PV module under partial shading.

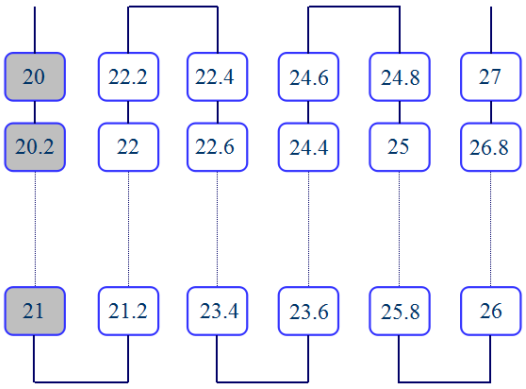

Figure 6. The partial shading condition of PV for a PV/T system.

3. MPPT Algorithm

MPPT algorithm is used for finding the current, the voltage, or the duty cycle corresponding to the maximum power, keeping the PV work on the MPP. This paper applies the GSO algorithm to the PV for the PV/T application. In order to evaluate the performance of this method, the P and O and FOCVT methods are applied for comparison.

3.1. The Proposed GSO-Based MPPT

This algorithm uses glowworms with a luminescent quantity, called luciferin, as their agents. In the beginning, glowworms, as initial solutions, are randomly distributed in the problem space, then they move to a brighter state in their own sensor range. Finally, they gather around the brightest ones, which correspond to the optimized solution of the problem. There are three phases in this process: luciferin update phase, movement phase, and the local-decision range update phase [23].

3.1.1. Luciferin Update Phase

The value of luciferin glowworms carry mainly depends on the objective function value of the current position. The formula for updating luciferin is given by:

$$I_i(t+1) = (1-\rho) * I_i(t) + \gamma * F(x_i(t+1)) \tag{10}$$

where ρ is the luciferin decay constant ($0 < \rho < 1$) set as 0.4, $(1-\rho) * I_i(t)$ to simulate the decay of the luciferin with time. γ is the luciferin enhancement constant set as 0.6, $I_i(t)$ and $I_i(t+1)$ are the luciferins at iterations t and $t+1$, respectively, and $F(x_i(t+1))$ represents the objective function which is the output power of the PV module in this paper, given by:

$$F = P_{pv} = V_{PV} * I \tag{11}$$

where V_{PV} is the total voltage of the PV cells in series. The voltage of each PV cell can be expressed as a function of the current I by deriving from Equations (1) to (8) in Section 2. Thus, F is the function of solar irradiation S, the current I, and the temperature T. In this study, the temperature distribution is set as shown in Figure 3, I is the parameter to be optimized through this algorithm, which is regarded as the location of the glowworm, and S is the input variable.

3.1.2. Movement Phase

Each agent decided to move to a superior individual according to a probability mechanism. The probability of the agent i moving to the agent j is calculated by:

$$p_{ij} = \frac{I_j(t) - I_i(t)}{\sum\limits_{m \in N_i(t)} I_m(t) - I_i(t)} \tag{12}$$

where $N_i(t)$ is the neighborhood group of the agent i:

$$N_i(t) = \left\{ j : d_{i,j}(t) < r_d^i, I_i(t) < I_j(t) \right\} \tag{13}$$

$d_{i,j}(t) = \|x_i - x_j\|$ is the Euclidean distance between glowworms i and j at iteration t. r_d^i represents the variable neighborhood range associated with glowworm i at time t.

Glowworms are attracted by neighbors that glow brighter; that is, glowworms will move to the neighbors that have larger luciferin values than the other neighbors. The movement is decided by the probability given by Equation (12). If $p_{ij0}(t) = \max\limits_{j}(p_{ij}(t))$, set the position of glowworm i equal to the position of glowworm j. Then glowworms update their position.

The movement update rule can be stated as follows:

$$x_i(t+1) = x_i(t) + s^*\left(\frac{x_j(t) - x_i(t)}{\|x_j(t) - x_i(t)\|}\right) \tag{14}$$

where s is the step size and $x_i(t)$ and $x_i(t+1)$ are the locations of agent i at iteration t and $t+1$, respectively.

3.1.3. Local-Decision Range Update Phase

The decision radius should be updated according to the number of individuals in the current range:

$$r_d^i(t+1) = \min\left\{r_s, \max\left\{0, r_d^i(t) + \beta^*(n_t - |N_i(t)|)\right\}\right\} \quad (15)$$

where β is the variation coefficient of the decision radius and n_t is the number of individuals with high luciferin values in the local-decision range.

The flowchart of this algorithm is shown in Figure 7.

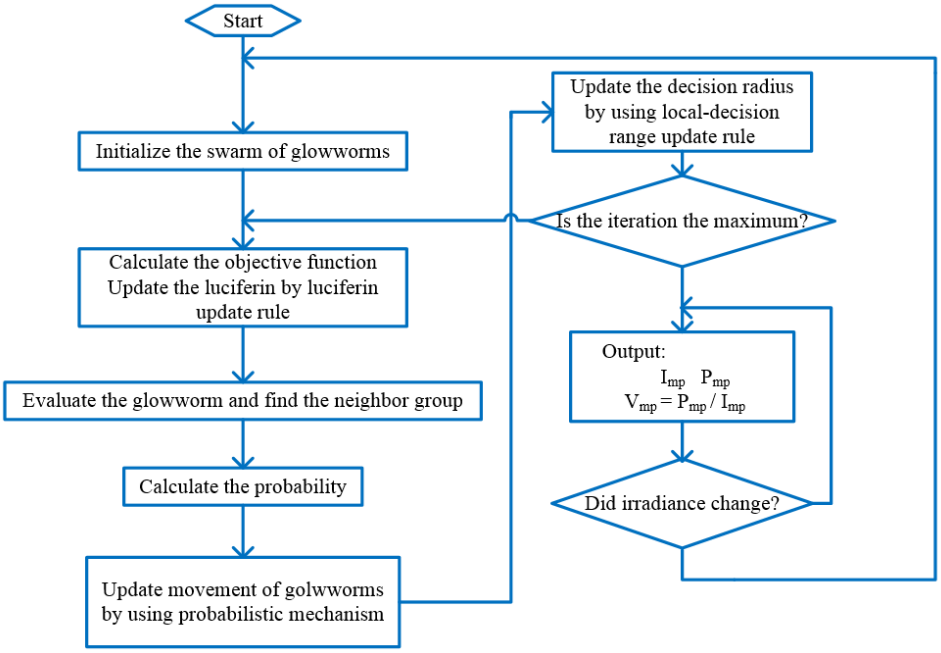

Figure 7. The flowchart of the glowworm swarm optimization (GSO) algorithm.

The algorithm parameters work well for a wide range of simulation scenarios and that only n and r_s are parameters that influence the algorithm's behavior [23]. Therefore, if the setting conditions are changed, these algorithm parameters will remain the same and do not need to be specifically tuned for every problem. Only n and r_s need to be selected to reduce the computing time and obtain higher peak-capture levels. The values of maximum iteration number and glowworm number used in the simulation of the GSO algorithm are set as 20 and 50 respectively.

3.2. Perturbation and Observe Algorithm

The traditional perturb and observe algorithm imposed a fixed-size disturbance on the control variables (voltage), and judged the next direction of the disturbance by observing the change of the power. In this method, the operating voltage is perturbed in a given direction; if the power increased (the operating point is moving towards to the MPP), the direction would be maintained, otherwise the direction would be the opposite. This method is impossible to considerate of the tracking efficiency and the steady state accuracy at the same time. In this paper, the step-size is set 0.5 V. The flow chart of the P and O algorithm is shown in Figure 8. If $P > P_{old}$, it means that the operating point is moving towards the MPP. Further voltage perturbations will be provided in the same direction as earlier in order to move operating point much closer to the MPP. If $P < P_{old}$, it means that the operating point is moving away from the MPP. Further voltage perturbations will be provided in the reverse direction in order to move operating point much closer to the MPP.

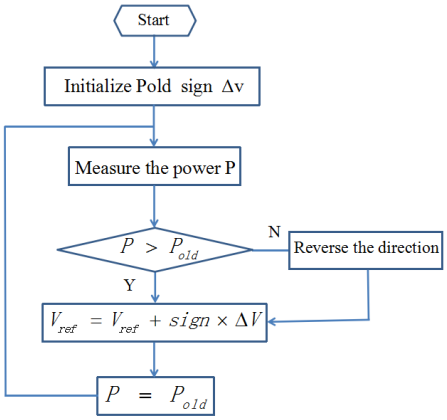

Figure 8. The flowchart of the perturbation and observe (P and O) algorithm.

3.3. Fractional Open-Circuit Voltage Technique

In this method, the voltage at the MPP is considered proportional to the open-circuit voltage of the PV. The relation is given by:

$$V_{mp} = K_v \cdot V_{oc} \tag{16}$$

where V_{mp} is the voltage corresponding to MPP, K_v is the coefficient of proportionality, usually ranging from 0.65 to 0.8. V_{oc} is the open-circuit voltage which can be calculated by analyzing the PV system.

4. Simulation Results

In order to compare the tracking performance of different methods mentioned above, the PV system is simulated in MATLAB/Simulink (R2015b, MathWorks, Natick, MA, USA). The system consist of a PV module, a DC-DC boost converter, a battery, the MPPT algorithm, and the pulse width modulation (PWM) module. The boost converter is used for MPPT to adjust the operating voltage by using PWM technique to control the opening and closing of the metal-oxide semiconductor field-effect transistor (MOSFET) switch at 10 kHZ. The inductor is set to 10 mH. The PWM technique uses the deviation of the V_{mp} and V_{PV} to form the closed-loop control. The structure diagram with the GSO algorithm is shown in Figure 9. In order to the study the performance and the suitable occasion of the proposed method, the simulation is implemented in the following cases:

Case 1: Gradient temperature distribution condition
Case 2: Fast variation in solar irradiation
Case 3: Partial shading condition
Case 4: Variation in the degree of shading.

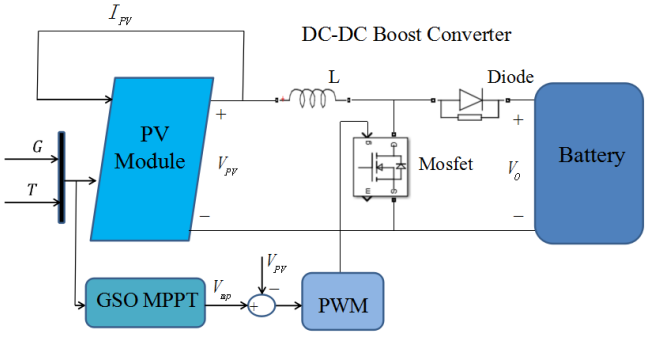

Figure 9. The structure diagram of the system. PWM: pulse width modulation; and MPPT: maximum power point tracking.

4.1. Gradient Temperature Distribution Condition

In this condition, the solar irradiance is supposed to be constant ($S = 1000\,\mathrm{W/m^2}$), while the temperature distribution of the PV module for PV/T system is shown in Figure 3. The simulation results show that the proposed GSO and the FOCVT methods can rapidly track the MPP in comparison with the P and O algorithm shown in Figure 10. The output power of PV module can reach a steady state in 0.0018 s by using the GSO and FOCVT methods in less than half of the settling time by using the P and O algorithm.

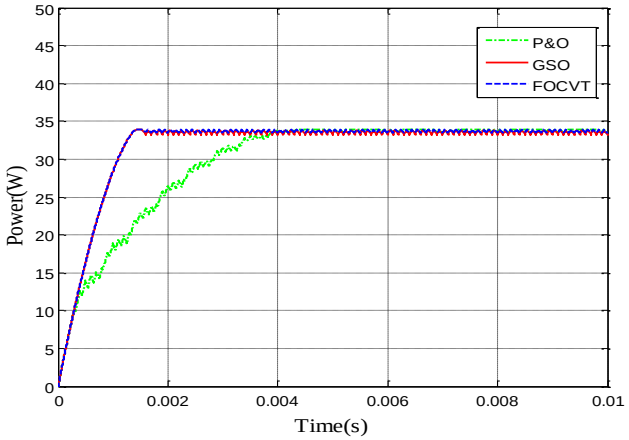

Figure 10. Output power under a gradient temperature distribution.

4.2. Fast Variation in Solar Irradiation

The temperature is assumed to be constant ($T = 25\,^{\circ}\mathrm{C}$), while there is a fast variation in the solar irradiation, as shown in Figure 11.

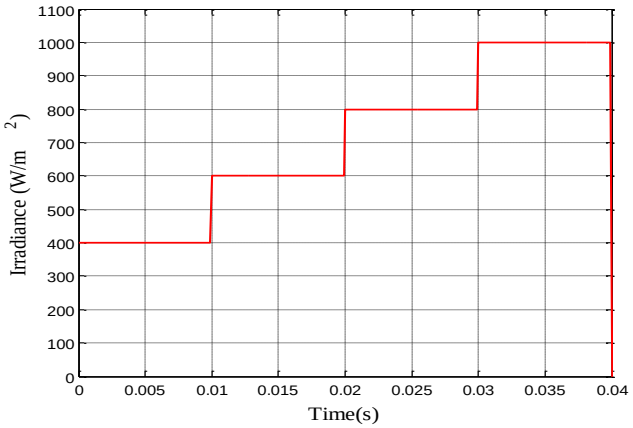

Figure 11. Variation of the solar irradiation.

This shows that the GSO algorithm and the FOCVT method can rapidly and correctly track the MPP under the condition of fast variation in solar irradiation in comparison with the P and O algorithm, as shown in Figure 12. As Figure 12 shows, it is obvious that the GSO algorithm can improve the maximum tracking power by 8% and 13.3% compared to the conventional P and O-based MPPT controller, respectively, when the solar irradiation changes from 600 $\mathrm{W/m^2}$ to 800 $\mathrm{W/m^2}$ at 0.02 s and from 800 $\mathrm{W/m^2}$ to 1000 $\mathrm{W/m^2}$ at 0.03 s, respectively. It can be seen that the GSO algorithm has the better steady-state performance than the FOCVT method. The steady state errors of using P and O will increase obviously with the solar irradiation increase. When the solar irradiation is 600 $\mathrm{W/m^2}$,

the RMSE of the output power by using P and O, GSO, and FOCVT are 0.9623, 0.4528, and 0.5701, respectively. It can be seen that the GSO algorithm has the better steady-state performance than the FOCVT and P and O methods.

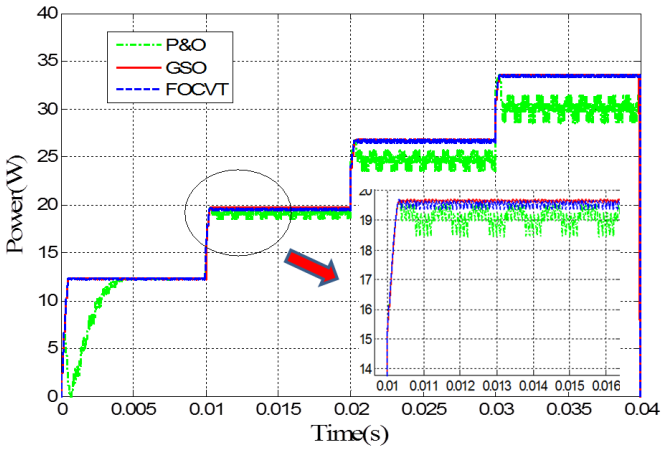

Figure 12. Output power under variable solar irradiation.

4.3. Partial Shading Condition

Under this condition, the temperature distribution and the shaded condition are shown in Figures 3 and 6, respectively. The solar irradiance of the shaded part is 600 $W/m^2$and that of the other part is normal ($S = 1000\,W/m^2$). It is obvious that the GSO algorithm can determine the GMPP in this condition, whereas the P and O and FOCVT algorithms converge to the LMPP from Figure 13. The GSO algorithm can improve the output power value by 12.5% compared to P and O- and FOCVT-based MPPT controllers under partial shading conditions. In addition, the P and O algorithm has a slow speed and greater fluctuation in the steady state.

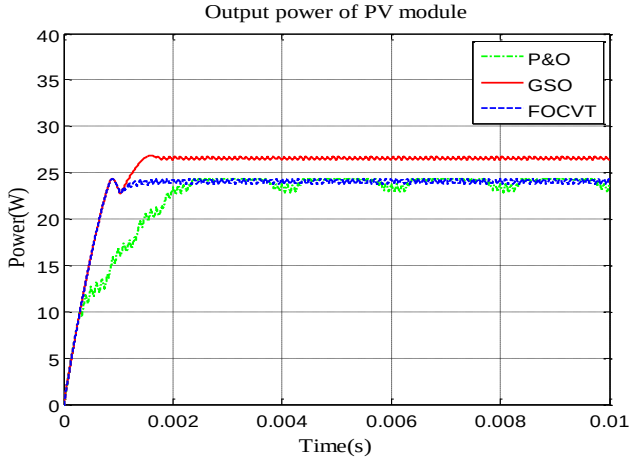

Figure 13. Output power under partial shading.

4.4. Variation in the Degree of Shading

Under this condition, the situation of the temperature distribution and shading are the same with case 3, however the solar irradiance of the shaded part changes, as shown in Figure 14. The solar irradiance of the other part is normal ($S = 1000\,W/m^2$). It is can be seen that the GSO algorithm can rapidly track the GMPP even when the shading degree varies, whereas the FOCVT method converge to the LMPP, the P and O algorithm diverged from the MPP in the limited time, as shown in Figure 15.

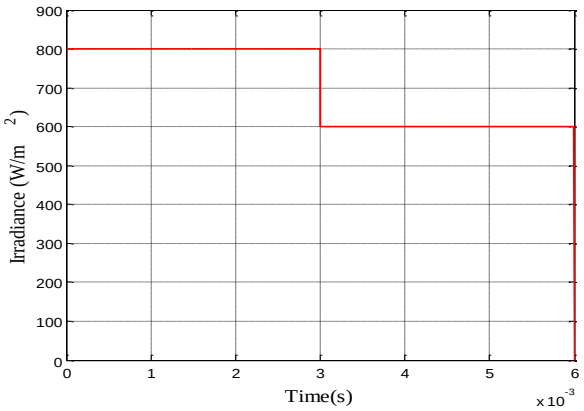

Figure 14. The solar irradiation of the shading part.

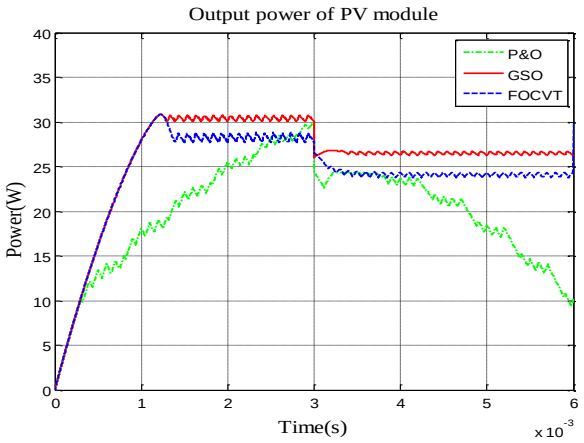

Figure 15. Output power under the variable degree of shading.

5. Conclusions

In this paper, a novel MPPT method based on the GSO algorithm is proposed and its performance is compared with P and O and FOCVT methods. The simulations used three different methods and are implemented through MATLAB/Simulink under four conditions (gradient temperature distribution condition, fast variation in solar irradiation, partial shading condition, and variation in the degree of shading). The output power of the photovoltaic (PV) system is affected by the external solar irradiation and its own temperature. Additionally, there will be multiple peaks in the P-I curves under the partial shading condition. In addition, the non-uniform temperature distribution appears on PV for PV/T applications. Taking into account the superiority in multi-peak function optimization, the GSO is applied to the MPPT control algorithm. It is confirmed by a simulation study that the GSO algorithm performs better than P and O and FOCVT. It can track the real MPP under different solar irradiation and temperature distributions with high accuracy, as well as partially-shaded conditions. However, the P and O and FOCVT will converge into the LMPP under the partially-shaded condition. Moreover, the GSO algorithm has a better time response in comparison with the P and O algorithm, and its convergence speed is higher than the two other algorithms.

Acknowledgments: The study was sponsored by the National Science Foundation of China (Grant Nos. 51408578, 51605464, 51476159), Anhui Provincial Natural Science Foundation (1508085QE96, 1508085QE83).

Author Contributions: Yi Jin designed and developed the main parts of the research work, including simulation model and analyses of the obtained results. Wenhui Hou contributed in simulation and writing parts. Guiqiang Li contributed in theoretical analysis. Xiao Chen also involved in verifying the work and actively contributed to finalize the manuscript.

Conflicts of Interest: The authors declare no conflict of interest.

Nomenclature

A	Diode ideality factor	q	Electronic charge (C)
d_{ij}	Euclidean distance between i and j	r_d^i	Local decision radius
E_g	Band gap energy of semiconductor	r_s	Largest sensing radius
F	Objective function	R_{sh}	Parallel resistance
I	PV cell output current (A)	R_s	Series resistance
I_d	Diode current (A)	s	Movement step size
I_i	Luciferin of glowworm i	S	Solar radiation (W/m^2)
I_{mp}	Current corresponding to the MPP	t	Iteration number
I_O	Diode reverse saturation current (A)	T	Temperature
I_{sh}	Parallel resistance current (A)	T_c	Operating temperature (K)
I_{ph}	Light-generated current (A)	T_r	Reference temperature (K)
I_{ro}	Diode reverse saturation current at STC (A)	U	PV cell output voltage (V)
I_{sc}	Short-circuit current (A)	U_d	Diode voltage
k	Boltzmann's constant (J/K)	V_{PV}	Voltage of the PV module
K_v	The coefficient of the proportionality	V_{mp}	Voltage corresponding to the MPP
n_t	Number of outstanding individuals	V_o	Boost converter output voltage (V)
$N_i(t)$	Neighborhood of agen	V_{oc}	Open-circuit voltage
P	PV cell output power	x_i	Location of glowworm i Greek symbols
P_{ij}	Probability of glowworm i moving to j	α	The current temperature coefficient
$P_{\max}$	PV maximum power (W)	β	Variation coefficient of decision radius
P_{ij}	Probability of glowworm i	γ	Luciferin enhancement constant
P_{pv}	PV module output power (W)	ρ	Luciferin decay constant

References

1. Sahoo, S.K. Renewable and sustainable energy reviews solar photovoltaic energy progress in India: A review. *Renew. Sustain. Energy Rev.* **2016**, *59*, 927–939. [CrossRef]
2. Subudhi, B.; Pradhan, R. A comparative study on maximum power point tracking techniques for photovoltaic power systems. *IEEE Trans. Sustain. Energy* **2013**, *4*, 89–98. [CrossRef]
3. Qin, L.; Lu, X. Matlab/Simulink-based research on maximum power point tracking of photovoltaic generation. *Phys. Procedia* **2012**, *24*, 10–18. [CrossRef]
4. Bendib, B.; Belmili, H.; Krim, F. A survey of the most used MPPT methods: Conventional and advanced algorithms applied for photovoltaic systems. *Renew. Sustain. Energy Rev.* **2015**, *45*, 637–648. [CrossRef]
5. Jubaer, A.; Zainal, S. An improved perturb and observe (P&O) maximum power point tracking (MPPT) algorithm for higher efficiency. *Appl. Energy* **2015**, *150*, 97–108.
6. Elgendy, M.A.; Zahawi, B.; Atkinson, D.J. Assessment of perturb and observe MPPT algorithm implementation techniques for PV pumping applications. *IEEE Trans. Sustain. Energy* **2012**, *3*, 21–33. [CrossRef]
7. Bangyin, L.; Shanxu, D.; Fei, L.; Pengwei, X. Analysis and improvement of maximum power point tracking algorithm based on incremental conductance method for photovoltaic array. In Proceedinngs of the Seventh International Conference on Power Electronics and Drive Systems, Bangkok, Thailand, 27–30 November 2007; pp. 637–641.
8. Mohammed, S.S.; Devaraj, D. Simulation of Incremental Conductance MPPT based two phase interleaved boost converter using MATLAB/Simulink. In Proceedinngs of the IEEE International Conference Electrical, Computer and Communication Technologies (ICECCT), Coimbatore, India, 5–7 March 2015; pp. 1–6.
9. Sivakumar, P.; Kader, A.A.; Kaliavaradhan, Y.; Arutchelvi, M. Analysis and enhancement of PV efficiency with incremental conductance MPPT technique under non-linear loading conditions. *Renew. Energy* **2015**, *81*, 543–550. [CrossRef]

10. Chen, P.C.; Chen, P.Y.; Liu, Y.H.; Chen, J.H.; Luo, Y.F. A comparative study on maximum power point tracking techniques for photovoltaic generation systems operating under fast changing environments. *Sol. Energy* **2015**, *119*, 261–276. [CrossRef]
11. Bayod-Rújula, Á.A.; Cebollero-Abián, J.A. A novel MPPT method for PV systems with irradiance measurement. *Sol. Energy* **2014**, *109*, 95–104. [CrossRef]
12. Rezk, H.; Hasaneen, E.S. A new MATLAB/Simulink model of triple-junction solar cell and MPPT based on artificial neural networks for photovoltaic energy systems. *Ain Shams Eng. J.* **2015**, *6*, 873–881. [CrossRef]
13. Zaghba, L.; Terki, N.; Borni, A.; Bouchakour, A. Intelligent control MPPT technique for PV module at varying atmospheric conditions using MATLAB/SIMULINK. In Proceedings of the 2014 International Renewable and Sustainable Energy Conference (IRSEC), Ouarzazate, Morocco, 17–19 October 2014; pp. 661–666.
14. Guenounou, O.; Dahhou, B.; Chabour, F. Adaptive fuzzy controller based MPPT for photovoltaic systems. *Energy Convers. Manag.* **2014**, *78*, 843–850. [CrossRef]
15. Chen, Y.T.; Jhang, Y.C.; Liang, R.H. A fuzzy-logic based auto-scaling variable step-size MPPT method for PV systems. *Sol. Energy* **2016**, *126*, 53–63. [CrossRef]
16. Gounden, N.A.; Peter, S.A.; Nallandula, H.; Krithiga, S. Fuzzy logic controller with MPPT using line-commutated inverter for three-phase grid-connected photovoltaic systems. *Renew. Energy* **2009**, *34*, 909–915. [CrossRef]
17. Kofinas, P.; Dounis, A.I.; Papadakis, G.; Assimakopoulos, M.N. An Intelligent MPPT controller based on direct neural control for partially shaded PV system. *Energy Build.* **2015**, *90*, 51–64. [CrossRef]
18. Hadji, S.; Gaubert, J.P.; Krim, F. Theoretical and experimental analysis of genetic algorithms based MPPT for PV systems. *Energy Procedia* **2015**, *74*, 772–787. [CrossRef]
19. Sarvi, M.; Ahmadi, S.; Abdi, S. A PSO-based maximum power point tracking for photovoltaic systems under environmental and partially shaded conditions. *Prog. Photovolt. Res. Appl.* **2015**, *23*, 201–214. [CrossRef]
20. Soufyane Benyoucef, A.; Chouder, A.; Kara, K.; Silvestre, S. Artificial bee colony based algorithm for maximum power point tracking (MPPT) for PV systems operating under partial shaded conditions. *Appl. Soft Comput.* **2015**, *32*, 38–48. [CrossRef]
21. Larbes, C.; Cheikh, S.M.A.; Obeidi, T.; Zerguerras, A. Genetic algorithms optimized fuzzy logic control for the maximum power point tracking in photovoltaic system. *Renew. Energy* **2009**, *34*, 2093–2100. [CrossRef]
22. Sundareswaran, K.; Palani, S. Application of a combined particle swarm optimization and perturb and observe method for MPPT in PV systems under partial shading conditions. *Renew. Energy* **2015**, *75*, 308–317. [CrossRef]
23. Krishnanand, K.N.; Ghose, D. Glowworm swarm optimization for simultaneous capture of multiple local optima of multimodal functions. *Swarm Intell.* **2009**, *3*, 87–124. [CrossRef]
24. Singh, A.; Deep, K. New variants of glowworm swarm optimization based on step size. *Int. J. Syst. Assur. Eng. Manag.* **2015**, *6*, 286–296. [CrossRef]